ISSN 1023-1935, Russian Journal of Electrochemistry, 2017, Vol. 53, No. 9, pp. 1054–1060. © Pleiades Publishing, Ltd., 2017.
Published in Russian in Elektrokhimiya, 2017, Vol. 53, No. 9, pp. 1183–1192.

Electrochemical Oxidation of Formic Acid at Carbon Supported Pt Coated Rotating Disk Electrodes[1, 2]

Azam Sayadi and Peter G. Pickup*

Department of Chemistry, Memorial University, St. John's, Newfoundland and Labrador, A1B 3X7 Canada

**e-mail: ppickup@mun.ca*

Received October 14, 2016; in final form, November 20, 2016

Abstract—The effect of electrode rotation on the oxidation of formic acid in aqueous sulphuric acid has been investigated at a glassy carbon electrode coated with a carbon supported Pt catalyst. Substantial mass transport effects were observed in cyclic voltammetry, steady-state measurements at constant potential, and chronoamperometry. However, a purely mass transport limited current was not observed under any conditions because of a decrease in the kinetic current at high potentials due to Pt oxide formation. Steady-state measurements, and currents from the cathodic scans in cyclic voltammetry, gave linear Koutecky–Levich plots with slopes in agreement with the literature diffusion coefficient. However, non-linearity and inaccurate slopes were observed for anodic scans and chronoamperometry. This has been shown to be due to small increases in the kinetic current with increasing rotation rate. Accurate kinetic currents can be obtained by applying the Koutecky–Levich equation at each rotation rate and use of the known mass transport limited current.

Keywords: formic acid, rotating disk electrode, electrocatalysis, electron transfer kinetics, supported platinum catalyst, mass transport

DOI: 10.1134/S1023193517090117

1. INTRODUCTION

The electrochemical oxidation of formic acid is the simplest process for the oxidation of an organic molecule to carbon dioxide and therefore serves as an important model for understanding the fundamental steps in the electro-oxidation of organic fuels. Formic acid fuel cells are currently being developed for portable applications [1, 2], and methanol fuel cell technology is now well developed [3, 4].

Fundamental studies of formic acid oxidation have focussed on the use of Pt and Pt-based electrodes and catalysts, and there is now a good understanding of the mechanistic details [1, 5, 6]. Formic acid oxidation at Pt proceeds through two parallel pathways, direct and indirect, which both occur following the adsorption of formic acid onto an active site on the Pt surface. In the direct pathway (Eq. (1)), formic acid is oxidized directly to carbon dioxide through a dehydrogenation mechanism. On the other hand, the indirect pathway (Eq. (2)) involves dehydration of the adsorbed formic acid molecule to form adsorbed carbon monoxide (CO_{ads}), which is a stable intermediate at low potentials. The resulting CO_{ads} can accumulate on the Pt surface and partially block (poison) formic acid adsorption, which inhibits both pathways for its oxidation. The second step in the indirect pathway, oxidation of CO_{ads} to CO_2, only occurs at a significant rate when the Pt surface begins to oxidize to Pt–OH at potentials above ca. 0.5 V vs. SHE.

$$\begin{aligned} &HCOOH(aq) \rightarrow HCOOH_{ads} \\ &\rightarrow 2H^+ + 2e + CO_2, \end{aligned} \quad (1)$$

$$\begin{aligned} &HCOOH(aq) \rightarrow HCOOH_{ads} \\ &\rightarrow CO_{ads} + H_2O \rightarrow 2H^+ + 2e + CO_2. \end{aligned} \quad (2)$$

The kinetics of these processes, and the activities of different catalysts, are generally investigated by cyclic voltammetry and chronoamperometry. The effects of mass transport have been assumed to be negligible in most cases, which is reasonable for most flat electrodes. However, highly active electrode materials and thick catalytic layers produce much larger current densities, which can result in a significant reduction in the current due to concentration polarization (mass transport) [7, 8]. In such circumstances, rotating disk voltammetry (RDV) is generally used to separate the

[1] This paper is the authors' contribution to the special issue of Russian Journal of Electrochemistry dedicated to the 100th anniversary of the birth of the outstanding Soviet electrochemist Veniamin G. Levich.

[2] The article is published in the original.

kinetically (i_k) and mass transport limited (i_{mt}) components of the overall current (i) through use of the Koutecky–Levich (K–L) equation (3) [9–12].

$$1/i = 1/i_k + 1/i_{mt}, \quad (3)$$

where $i_{mt} = 0.62nFAD^{2/3}\nu^{-1/6}C\omega^{1/2}$, n is the number of electrons transferred ($n = 2$), F is the Faraday constant, A is the electrode area, D is the diffusion coefficient (1.46×10^{-5} cm^2 s^{-1} for aqueous formic acid at 25°C [13]), ν is the kinematic viscosity (1.0×10^{-2} cm^2 s^{-1} for water), C is the concentration of the reactant and ω is angular velocity.

There are only a few reports on the effects of electrode rotation on formic acid oxidation, and we have found no analysis of the mass transport rate. Pavese and Solis have investigated oxidation of formic acid on a palladium ring electrode in acid and reported that the oxidation current decreased as a result of increasing the rotation rate [14]. This was attributed to the blocking of the electrode surface by strongly adsorbed intermediates, which is enhanced by the convective increase in the HCOOH concentration at the Pd surface [14]. Shin et al. found that the current at a Pt disk electrode decreased with increasing rotation rate, while poisoning of the electrode (i.e. accumulation of adsorbed, oxidizable intermediates—mainly CO_{ads}) decreased [15]. In contrast to these results at Pd and Pt disk electrodes, Casado-Rivera et al. reported normal RDV behavior and a linear K–L plot (i^{-1} vs. $\omega^{-1/2}$) for formic acid oxidation at an intermetallic PtBi electrode [7]. Matsumoto et al. reported RDV data for formic acid oxidation at electrodes coated with Pt black, Pd black, carbon supported PtRu, and intermetallic PtPb nanoparticles [8]. While the PtPb gave a linear K–L plot, there was significant curvature for the other catalysts. In addition, the slopes of the K–L plot were different for each catalyst. Heterogeneous charge-transfer rate constants were calculated from the intercepts of the K–L plots, but analysis of the slopes was not reported. A number of other electrochemical studies of formic acid oxidation have been made at rotating disk electrodes (RDE) using a single rotation rate [16–20], in order to minimize mass transfer limitations [19], supress re-deposition of Bi when a PtBi alloy electrode was used [16], or minimize the effect of local pH changes [20].

We report here on the effects of electrode rotation at a glassy carbon disk electrode coated with a commercial carbon supported Pt catalyst (Pt/C). The goal was to verify that the mass transport rate conformed to the Levich equation, and to explore how the kinetics varied with potential and time. By using Eq. (3) to obtain mass transport corrected kinetic currents, we have been able to observe the true rate of poisoning of the catalyst surface.

2. EXPERIMENTAL

2.1. Materials and Solutions

Formic acid (98–100% from Sigma Aldrich), sulfuric acid (95–98% from ACP Chemical), and deionized water were used to prepare solutions. The catalyst ink was prepared from a Nafion™ solution in a mixture of lower aliphatic alcohols (5.14% from DuPont), 1-propanol (J.T. Baker), and a commercial carbon supported platinum catalyst (20% Pt; Etek). The electrode was polished with an alumina slurry (0.3 μm, Sturbridge Metallurgical Services, Inc.).

2.2. Electrode Preparation

For catalyst ink preparation, a weighed amount of catalyst powder (ca. 28 mg mL^{-1}) was dispersed in a mixture of 1-propanol and Nafion solution homogenously in an ultrasonic bath for 3 h. The required amount of catalyst ink was applied onto the polished surface of a glassy carbon disk electrode (0.196 cm^2; Pine Instruments) with an Eppendorf micropipette and was allowed to dry at ambient temperature for ca. 30 min while it was rotated first at 100 rpm (ca. 15 min) and then at 600 rpm [21]. The catalyst layer contained ca. 1 mg cm^{-2} Pt/C (0.2 mg Pt cm^{-2}) and ca. 25% Nafion by mass.

2.3. Electrochemistry

All electrochemical measurements were conducted at ambient temperature (24–25°C) in a three-compartment glass cell using a catalyst coated glassy carbon electrode as the working electrode, a platinum wire as the counter electrode and a mercury sulfate electrode in 3.8 M sulfuric acid (Koslow; 635 mV vs. SHE) as a reference electrode. However, all potentials are given relative to the standard hydrogen electrode (SHE). An EG&G model 273A Potentiostat/Galvanostat and Pine Instruments ASR Analytical Rotator were used for rotating disk cyclic voltammetry, constant potential and pulsed potential experiments in a 0.1 M formic acid solution with 1 M sulfuric acid as the electrolyte. The solution was de-aerated by passing N_2 into the solution for 20 min prior to all experiments, and then over the surface of the solution continuously during the experiments. Cyclic voltammetry was performed at 10 mV s^{-1} between 0 and 1.24 V vs. SHE. For RDV, the first cathodic scan and second anodic scan are shown, since the first anodic scan was less reproducible due to variations in the coverage of adsorbed intermediates. The first anodic scan was used to clean and activate the electrode to produce a reproducible surface.

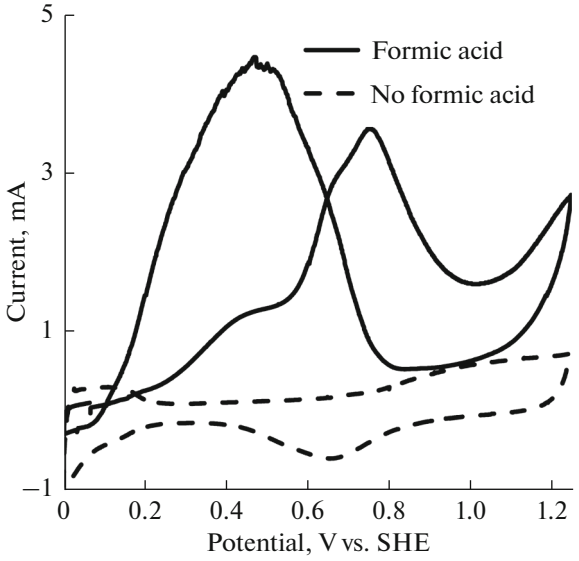

Fig. 1. Cyclic voltammograms (10 mV s^{-1}) of a stationary GC/Pt/C (1.04 mg cm^{-2}) electrode in 1 M H_2SO_4(aq) (dashed; the 2nd scan is shown), and with 0.1 M formic acid (solid; 1st scan from the open circuit potential of 0.06 V).

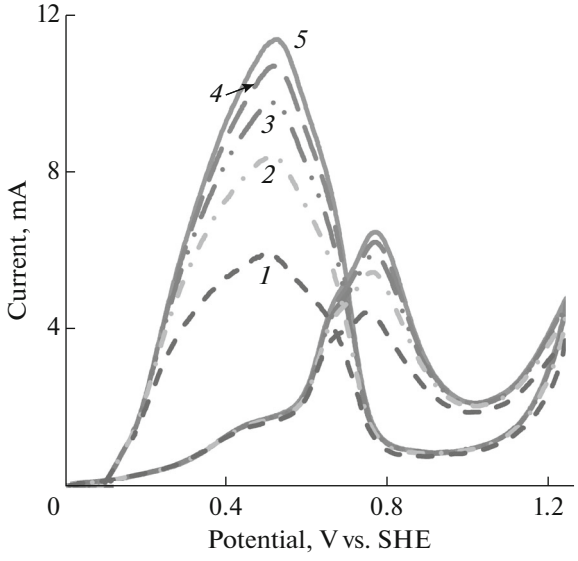

Fig. 2. Cyclic voltammograms (10 mV s^{-1}) of 0.1 M formic acid in 1 M H_2SO_4(aq) at a GC/Pt/C (1.04 mg cm^{-2}) electrode at 100 (*1*), 400 (*2*), 900 (*3*), 1600 (*4*), and 2500 (*5*) rpm. The 1st cathodic scan and 2nd anodic scan are shown.

3. RESULTS AND DISCUSSION

3.1. Rotating Disk Cyclic Voltammetry

Figure 1 shows cyclic voltammetry of the stationary Pt/C coated glassy carbon electrode in sulphuric acid solution in the absence and presence of formic acid. In the anodic scan, the oxidation current due to the direct pathway for formic acid oxidation commenced at 0.16 V and increased to a plateau at ca. 0.5 V. At higher potentials the oxidative removal of CO as CO_2 caused the current to increase to a peak at 0.75 V, where it is dominated by the direct pathway on the unblocked Pt surface [22]. At this point the increasing oxide coverage of the Pt surface limits the availability of sites for formic acid adsorption, and the current begins to decrease. In the cathodic scan, reduction of the oxide layer begins at ca. 0.8 V and the oxidation of formic acid then proceeds rapidly on the bare platinum sites that are formed. This results in a large anodic peak at ca. 0.5 V due primarily to the direct pathway.

In Fig. 2, cyclic voltammograms (CV) are shown for formic acid oxidation over a range of rotation rates. On the anodic scans, the current for formic acid oxidation at the CO poisoned surface (i.e. to ca. 0.55 V) is only slightly influenced by rotation of the electrode, while the current for the unblocked surface (>0.55 V) increases sharply with increasing rotation rate. The large anodic peak on the cathodic scan also depends strongly on rotation rate. Although these differences in the rotation rate dependence over the different regions of the voltammogram may appear to be significant, they can simply be accounted for by use of Eq. (3). When i_k is small, the kinetic term dominates. Consequently, the effect of changing i_{mt} becomes insignificant when i_k is less than ca. 10% of i_{mt}. In Fig. 2, i_{mt} increases from 9.8 mA at 100 rpm to 49 mA at 2500 rpm, and so the effect of increasing the electrode rotation rate is only significant when the current is above ca. 1 mA.

The rotating disk voltammograms in Fig. 2 are unusual in that they do not reach a constant, mass transport limited current at high potentials. This is due to a decrease in i_k at potentials above 0.75 V due to the formation of an oxide layer on the Pt surface. It can be seen that the current remains well below i_{mt} (<50%) at all rotation rates.

It is instructive to visualize how the current is affected by concentration polarization, to illustrate the above discussion and to assess the errors that arise if it is assumed that the measured current in the CV at the stationary electrode is the kinetic current (i.e. if it is assumed that there is no mass transport effect). To do this, the CVs at the stationary electrode and at 400 rpm were first corrected for the background current due to the charging and electrochemistry of the catalyst layer by subtracting the current at the stationary electrode in the absence of formic acid. Then the CV at 400 rpm was corrected for mass transport by using Eq. (3) to obtain i_k vs. potential. The results are shown in Fig. 3. The CVs at other rotation rates produced very similar i_k CVs, justifying the use of Eq. (3) to estimate i_k, and making the selection of the 400 rpm data arbitrary.

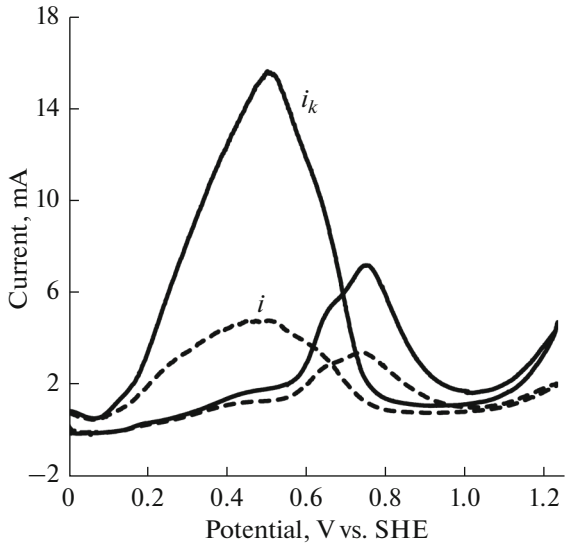

Fig. 3. Background corrected cyclic voltammogram (10 mV s^{-1}) of 0.1 M formic acid in 1 M H_2SO_4(aq) at a stationary GC/Pt/C (1.04 mg cm^{-2}) electrode (dashed) and i_k vs. potential from a background corrected voltammogram at 400 rpm (solid).

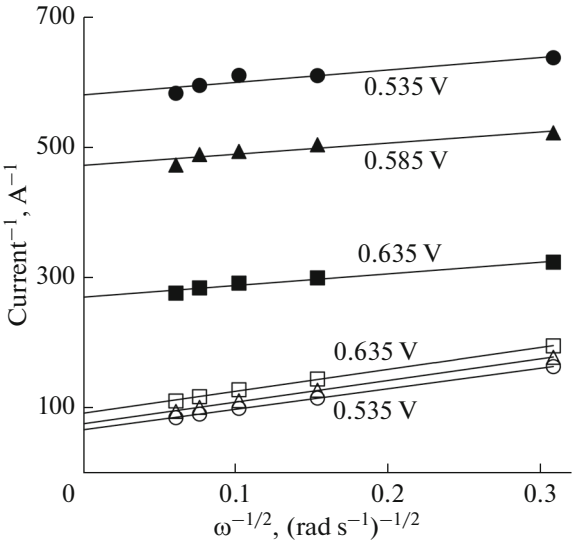

Fig. 4. Koutecky–Levich plots from background corrected cyclic voltammograms for oxidation of 0.1 M formic acid in 1 M H_2SO_4(aq) at a GC/Pt/C (1.04 mg cm^{-2}) electrode at 0.535 V (circles), 0.585 V (triangles) and 0.635 V (squares) on the anodic (solid points) and cathodic (open points) scans.

However, it should be noted that the background correction employed here is only approximate because the adsorbed intermediates change the electrochemistry of the Pt surface. This is most obvious in the hydrogen adsorption-desorption region below 0.25 V.

It can be seen from Fig. 3 that the CV at the stationary electrode gives a very poor approximation of the kinetic current, which represents the true activity of the catalyst layer. Consequently, Tafel plots of the CV currents would be very inaccurate, except at very low potentials, and comparisons of the CVs of different catalyst layers would be quite misleading.

The application of Eq. (3) to produce the mass transport corrected voltammogram in Fig. 3 is based on the assumption that the electron transfer kinetics are first order [9]. This was confirmed by analysis of voltammograms obtained for 0.2 to 1 M formic acid at a stationary electrode. Data at three potentials on the anodic scans and three on the cathodic scans gave an average reaction order of 0.99 ± 0.13. In order to further test the validity of Eq. (3) here, K–L plots were made using currents at various potentials on the anodic and cathodic scans of the voltammograms in Fig. 2, following background correction. Examples are shown in Fig. 4. These plots were linear and parallel for data collected during the cathodic scan, with slopes corresponding to $n = 2.08 \pm 0.08$, which is within experimental uncertainty of the value of $n = 2$ for oxidation of formic acid to CO_2. There was not a significant dependence of n on potential (Fig. 5). In contrast, data collected on the anodic scan gave nonlinear K–L plots (Fig. 4) with slopes that varied with potential. The apparent number of electrons transferred (Fig. 5) decreased with increasing potential from 4.7 to 1.2, which is clearly nonsensical. Although this failure of Eq. (3) for data on the anodic scan could be due to random errors, due to the very small differences in the current with changing rotation rate, the

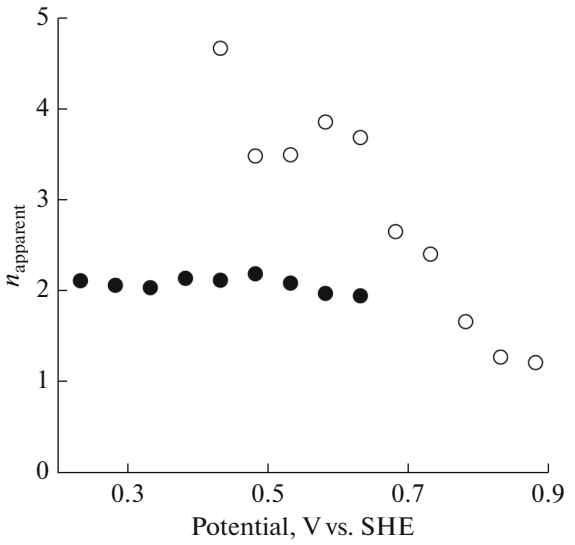

Fig. 5. Apparent number of electrons transferred ($n_{apparent}$) vs. potential for oxidation of 0.1 M formic acid in 1 M H_2SO_4(aq) at a GC/Pt/C (1.04 mg cm^{-2}) electrode, from anodic (open points) and cathodic (solid points) voltammetric scans.

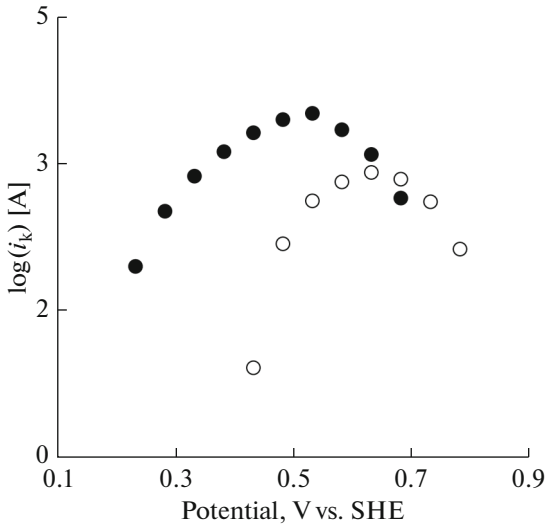

Fig. 6. Tafel plots for oxidation of 0.1 M formic acid in 1 M H_2SO_4(aq) at a GC/Pt/C (1.04 mg cm^{-2}) electrode, from the cathodic scans of cyclic voltammograms (solid) and from steady-state currents (open).

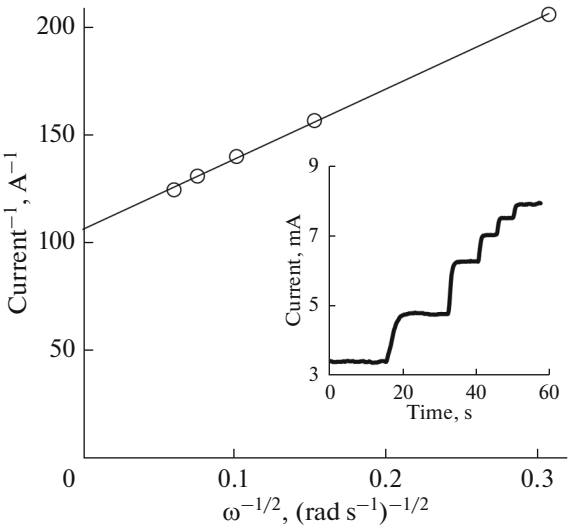

Fig. 7. Steady-state Koutecky–Levich plot for constant potential oxidation of 0.1 M formic acid in 1 M H_2SO_4(aq) at a GC/Pt/C (1.04 mg cm^{-2}) electrode at 0.635 V. Inset: current vs. time at 0.635 V and various rotation rates from 0 to 2500 rpm.

curvature indicates that there was also a systematic error. This is explored in Sections 3.2 and 3.3.

Kinetic currents (i_k) from the intercepts of the linear K–L plots for the cathodic scans are shown as a Tafel plot in Fig. 6. This clearly shows that i_k is lower at higher potentials, when there is an oxide layer on the electrode. The decrease in i_k at low potentials, as the potential was decreased during the cathodic scan, is due primarily to the decreasing overpotential. However, linear Tafel behaviour is not observed due to the increasing coverage of CO_{ads} on the Pt surface during the scan. Kinetic currents for the anodic scan are not shown because they would clearly be very inaccurate.

It should be noted that the kinetic currents reported here presumably include a component due to diffusion of formic acid into the thick catalyst layers that have been employed. This does not affect the validity of Eq. (3) [23], but does provide data that is most relevant to the use of thick catalyst layers in fuel cells. The intrinsic activity of the catalyst could be extracted if the mass transport characteristics of the catalyst layer were known [24].

3.2. Steady State Experiments

In addition to cyclic voltammetry, steady state rotating disk electrode (RDE) experiments were conducted in order to explore why linear K–L plots and reasonable *n* values were only obtained for the negative voltammetric scan. These experiments also provide data that is more relevant to applications, particularly in fuel cells, where there is a steady state coverage of CO_{ads}.

During these experiments, the current was recorded at a constant potential as the rotation rate was increased in a series of steps, as illustrated in Fig. 7 (inset). This type of experiment was repeated over a range of potentials, with a cyclic scan between 0 and 1.235 V between each experiment to clean and activate the electrode. K–L plots of the steady state currents showed good linearity (e.g. Fig. 7), with slopes that were independent of potential and correspond to the transfer of 2.00 ± 0.06 electrons. Kinetic currents from the intercepts are compared with those from CV in Fig. 6. In the low potential region (0.4 to 0.6 V), they are much lower because the Pt is heavily poisoned with CO_{ads} at steady state. However, the CV and steady state values converge in the high potential region where the CO_{ads} coverage is lower and doesn't change with time. In fact, the steady-state value is higher than the CV value at 0.685 V because of the hysteresis in the oxide coverage, since the oxide layer reduces at lower potentials than for its formation.

Since the steady state measurements were conducted in the order of increasing potential, and show normal K–L behaviour, the anomalous K–L behaviour in cyclic voltammetry does not appear to be due to the scan direction, per se. Instead, it would appear to be due to the effect of time, which is absent in the steady state measurements. Previously, it has been reported that the rate of CO_{abs} accumulation on the Pt surface decreases as the rotation rate is increased [15]. This would adequately explain the curvature of the K–L plots, where the current is higher than it should be at high rotation rates.

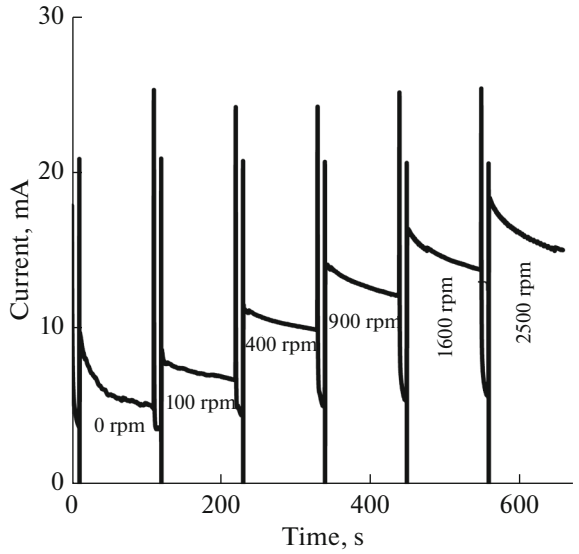

Fig. 8. Chronoamperometry at 0.435 V for the oxidation of 0.1 M formic acid in 1 M H_2SO_4(aq) at a GC/Pt/C (1.25 mg cm^{-2}) electrode at 0, 100, 400, 900, 1600, and 2500 rpm. The potential was stepped to 1.235 V for 10 s while the rotation rate was changed.

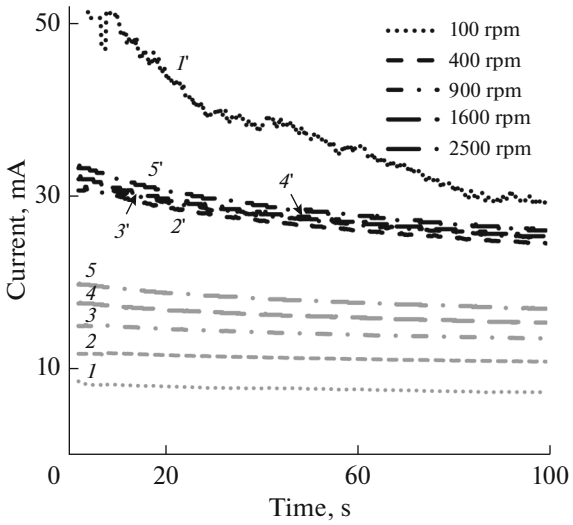

Fig. 9. Currents (i, grey) and kinetic currents (i_k, black) vs. time for oxidation of 0.1 M formic acid in 1 M H_2SO_4(aq) at 0.485 V at a GC/Pt/C (1.25 mg cm^{-2}) electrode at 100 (*1*), 400 (*2*), 900 (*3*), 1600 (*4*), and 2500 (*5*) rpm. The potential was stepped to 1.235 V for 10 s while the rotation rate was changed. Data for the first 2 s are omitted because of inaccuracy due to the time constant of the cell.

3.3. Potential Step Experiments

One of the disadvantages of cyclic voltammetry is that the current at any potential is affected by the history of the electrode at previous potentials. Also, in both CV and steady state experiments the electrode is exposed to poisoning for relatively long periods of time. Poisoning is affected not only by the potential but also the time at that potential, or its rate of change [5, 25]. To evaluate the effect of time on the kinetics of formic acid oxidation, a pulsed potential procedure [26] was used, in order to clean the electrode and restore it to a consistent state before measurements at each rotation rate and each potential. During these experiments a high potential (1.235 V) was applied to the electrode for a short period of time (10 s) in order to remove CO_{ads} and form an oxide layer. The potential was then stepped to the desired lower potential in order to remove the oxide layer and initiate the oxidation of formic acid at the clean, and activated, Pt surface. This sequence of steps was repeated at different rotation rates at each test potential. Data for 0.435 V, which is close to the peak potential for the direct pathway, is shown in Fig. 8. It can be seen that the decay rate of the current decreased significantly when the electrode was rotated at 100 rpm, but then appears to increase with increasing rotation rate. This indicates that the rate of poisoning is influenced by the mass transport conditions, as previously reported for a Pt disk electrode [15].

Because of the dependence of the poisoning rate on rotation rate, K–L plots at different times following the step to the test potential were all slightly curved, and there were small variations in the slope with the measurement time. Consequently, accurate i_k values could not be obtained from K–L plots. Therefore, each i vs. t curve was converted directly to i_k vs. t by using Eq. (3). Results at 0.485 V, which were similar to those at 0.435 V, are shown in Fig. 9. It can be seen that the raw i vs. t curves give a misleading impression of the differences in the activities of the catalyst, and that the decay rate of the kinetic current is not dependent on the rotation rate from 400 to 2500 rpm. However, there is a small systematic increase in i_k with increasing rotation rate, which is consistent with the curvature seen in the K–L plots. This same trend was observed at all other potentials (from 0.385 to 0.635 V) that were employed. The data at 100 rpm are anomalous, and this can be attributed to experimental errors. There is greater uncertainly (noise) in i_k at low rotation rates because the measured current is closer to the mass transport limited current. At 100 rpm, i_{mt} was 9.8 mA, while i decreased from 8.9 to 7.3 mA. These relatively small differences between i and i_{mt} lead to large random and systematic errors in i_k. In addition, the thicker diffusion layer at 100 rpm takes longer to be established, which causes a systematic error at short times, and also results in more noise due to vibrations. Consequently, the i_k values obtained at 100 rpm should be regarded as unreliable.

The results in Fig. 9 further demonstrate the importance of mass transport corrections when conducting kinetic studies at high surface area catalysts. Even at very low potentials, the kinetic current is much

higher than the currents measured by cyclic voltammetry or chronoamperometry at a stationary electrode, unless there is severe poisoning.

4. CONCLUSIONS

Formic acid oxidation at an electrode coated with a layer of carbon supported Pt catalyst with 0.2 mg Pt cm^{-2} shows substantial mass transport limitations at potentials above 0.1 V vs. SHE unless there is severe poisoning due to adsorbed CO. Although pure mass transport control of the current has not been observed, the Koutecky–Levich equation can be applied to extract mass transport and kinetic parameters. However, changes in the kinetic current with changing rotation rate can cause plots of 1/current vs. $\omega^{-1/2}$ to be non-linear, with inaccurate slopes and intercepts. Under such conditions, the kinetic current can be calculated at each rotation rate by use of the known mass transport limited current.

ACKNOWLEDGMENTS

This work was supported by the Natural Sciences and Engineering Research Council of Canada and Memorial University.

REFERENCES

1. Jeon, H., Jeong, B., Joo, J., and Lee, J., *Electrocatalysis*, 2015, vol. 6, p. 20.
2. Rees, N.V. and Compton, R.G., *J. Solid State Electrochem.*, 2011, vol. 15, p. 2095.
3. Kumar, P., Dutta, K., Das, S., and Kundu, P.P., *Int. J. Energy Res.*, 2014, vol. 38, p. 1367.
4. Mallick, R.K., Thombre, S.B., and Shrivastava, N.K., *Renewab. Sustainab. Energy Rev.*, 2016, vol. 56, p. 51.
5. Boronat-Gonzalez, A., Herrero, E., and Feliu, J.M., *J. Solid State Electrochem.*, 2014, vol. 18, p. 1181.
6. Jiang, K., Zhang, H.X., Zou, S.Z., and Cai, W.B., *Phys. Chem. Chem. Phys.*, 2014, vol. 16, p. 20360.
7. Casado-Rivera, E., Gal, Z., Angelo, A.C.D., et al., *Chem. Phys. Chem.*, 2003, vol. 4, p. 193.
8. Matsumoto, F., Roychowdhury, C., DiSalvo, F.J., and Abruna, H.D., *J. Electrochem. Soc.*, 2008, vol. 155, p. B148.
9. Bard, A.J. and Faulkner, L.R., *Electrochemical Methods. Fundamentals and Applications*, 2nd ed., New York: Wiley, 2001.
10. Frumkin, A. and Aikazyan, E., *Dokl. Akad. Nauk SSSR*, 1955, vol. 100, p. 315.
11. Koutecky, J. and Levich, V., *Dokl. Akad. Nauk SSSR*, 1957, vol. 117, p. 441.
12. Frumkin, A. and Tedoradze, G., *Dokl. Akad. Nauk SSSR*, 1958, vol. 118, p. 530.
13. Albery, W.J., Greenwood, A.R., and Kibble, R.F., *Trans. Faraday Soc.*, 1967, vol. 63, p. 360.
14. Pavese, A. and Solis, V., *J. Electroanal. Chem.*, 1991, vol. 301, p. 117.
15. Shin, D., Kim, Y.R., Choi, M., and Rhee, C.K., *J. Electrochem. Sci. Technol.*, 2014, vol. 5, p. 82.
16. Tripkovic, A.V., Popovic, K.D., Stevanovic, R.M., et al., *Electrochem. Commun.*, 2006, vol. 8, p. 1492.
17. Ghosh, T., Zhou, Q., Gregoire, J.M., et al., *J. Phys. Chem. C*, 2010, vol. 114, p. 12545.
18. Lovic, J.D., Tripkovic, D.V., Popovic, K.D., et al., *J. Serb. Chem. Soc.*, 2013, vol. 78, p. 1189.
19. Bauskar, A.S. and Rice, C.A., *Electrochim. Acta*, 2013, vol. 107, p. 562.
20. Brimaud, S., Solla-Gullon, J., Weber, I., et al., *Chem. Electrochem.*, 2014, vol. 1, p. 1075.
21. Garsany, Y., Singer, I.L., and Swider-Lyons, K.E., *J. Electroanal. Chem.*, 2011, vol. 662, p. 396.
22. Grozovski, V., Solla-Gullon, J., Climent, V., et al., *J. Phys. Chem. C*, 2010, vol. 114, p. 13802.
23. Amarasinghe, S., Chen, T.Y., Moberg, P., et al., *Anal. Chim. Acta*, 1995, vol. 307, p. 227.
24. Gloaguen, F., Andolfatto, F., Durand, R., and Ozil, P., *J. Appl. Electrochem.*, 1994, vol. 24, p. 863.
25. Lovic, J.D., Tripkovic, A.V., Gojkovic, S.L.J., et al., *J. Electroanal. Chem.*, 2005, vol. 581, p. 294.
26. Grozovski, V., Climent, V., Herrero, E., and Feliu, J.M., *Phys. Chem. Chem. Phys.*, 2010, vol. 12, p. 8822.